

## Eco-friendly Synthesis of Gold Nanoparticles by Using *B. javanica Blume* Leaves Extract Encapsulated with Graphene Oxide for Selective Electrochemical Detection of Dopamine

R. karthik<sup>1</sup>, K. Saravanakumar<sup>2</sup>, Shen-Ming Chen<sup>1,\*</sup>, J. Vinoth Kumar<sup>2</sup>, Chia-Ming Lee<sup>1</sup>, Bih-Show Lou<sup>3,4\*</sup>, V. Muthuraj<sup>2</sup>, A. Elangovan<sup>5</sup>, S. Kulandaivel<sup>6</sup>

<sup>1</sup> Department of Chemical Engineering, National Taipei University of Technology, No. 1, Section 3, Chung-Hsiao East Road, Taipei 106, Taiwan, ROC.

<sup>2</sup> Department of chemistry, VHNSN College, Virudhunagar – 626001, Tamilnadu, India.

<sup>3</sup> Chemistry Division, Center for General Education, Chang Gung University, Taoyuan 333, Taiwan, ROC.

<sup>4</sup> Department of Nuclear Medicine and Molecular Imaging Center, Chang Gung Memorial Hospital, Taoyuan 333, Taiwan, ROC.

<sup>5</sup> Department of chemistry, Thiagarajar College, Madurai-625009, Tamilnadu, India.

<sup>6</sup> Department of Zoology & Microbiology, Thiagarajar College, Madurai-625009, Tamilnadu, India.

\* E-mail: [smchen78@ms15.hinet.net](mailto:smchen78@ms15.hinet.net), [blou@mail.cgu.edu.tw](mailto:blou@mail.cgu.edu.tw)

Received: 11 October 2016 / Accepted: 19 December 2016 / Published: 30 December 2016

---

A simple, facile, eco-friendly and rapid synthesis of gold nanoparticles (GNPs) derived from *B. javanica Blume* leaves extract (BJBLE) was successfully developed. The GNPs were formed within 40 sec and it was confirmed by UV-visible spectroscopy. The BJBLE acts as a (strong) reducing and (as well as) stabilizing agent. The Chemical constituents of BJBLE were studied by GC-MS. The prepared GNPs are spherical in shape and the particles size around 25 nm, which was confirmed by HR-TEM. The formation of GNPs and interaction between the plant extract was characterized by XRD and FT-IR. One step preparation of graphene oxide encapsulated GNPs (GO/GNPs) was confirmed by SEM and EDX spectrum. The electrochemical activities of the GO/GNPs modified electrode were characterized by CVs and DPV. The electrochemical results demonstrate notable electrocatalytic activity of the GO/GNPs modified glassy carbon electrode (GCE) towards dopamine detection. The GO/GNPs modified GCE displayed a wide linear range with a low detection limit of 0.03  $\mu\text{M}$  and good selectivity towards dopamine even in the presence of biologically co-interfering substances. The above results suggested that the GO/GNPs modified GCE is very promising and active electrode material for the detection of dopamine for pharmaceutical and clinical applications.

---

**Keywords:** Gold nanoparticles, Graphene oxide, *B. javanica Blume*, Dopamine.

## 1. INTRODUCTION

Dopamine (DA) belongs to the families of catecholamine and phenethylamine in both peripheral nervous and mammalian central nervous system, which plays a significant role in the human brain and body such as neurotransmission, metabolism, emotional expression and mental activity [1]. The main function as a DA is neurotransmitter in central nervous system, cardiovascular and hormonal system. However, the abnormal metabolism or high either low level concentration of DA in the region of the brain the activity would be difficult and dangerous causes diseases such as parkinson's disease [2], senile, dementia, HIV infection [2], Harrington's and Schizophrenia disease [3]. Hence, an aforementioned reason, the rapid and selective determination of DA is necessary. So far, a number of traditional methods have been developed towards DA detection, including fluorescent spectrometry [4–6] and chromatography [7]. But these techniques are high cost, that instruments are operated by highly skilled technicians and time consuming methods. The electrochemical techniques are widely used for the sensitive determination of DA, because of low cost, high sensitivity, simplicity, reproducibility, selectivity and short measurement time [8–11]. In order to realize the sensitive detection of DA, the modified electrodes with metal nanoparticles (MNPs), metal oxides, conducting polymers and carbon related nanomaterials etc., have been mostly used for the sensitive and selective detection of DA in the electrochemical field [12–18].

Nanoparticles made of various noble metals have been received a vital consideration over the recent years, as they can be applied in chemistry, physics, biology, medicine and material science [19]. Particularly, plant mediated biological synthesis of noble and transition metal nanoparticles is currently focused hearted research area, owing to the benefits of rapid, facile, large scale production, energy-efficient, biocompatible, environmentally conscious, avoid toxic chemicals and cost effective reagents when compared to other physical and chemical phenomenon [20, 21]. Syntheses of different MNPs such as Ag, Au, Pt, Cu and Ru are prepared via biological route was also reported previously [22–24]. Among these MNPs, gold nanoparticles (GNPs) find applications in drug delivery, tissue/tumor imaging and photothermal therapeutic contexts owing to their extraordinary behavior and their broad spectrum of physical, chemical and optical properties [25]. The presence of bio-molecule in the plant extract that can be used as a reducing agents for reduce the metal ion to metal nanoparticles ( $\text{Au}^{3+}$  to  $\text{Au}^0$ ) and stabilize them. Varieties of plant extract have been used as reducing agents as well as capping agent for preparation of GNPs and are reported previously [26–33]. There is still a lot of attention paid to this field because of the high potential of plants in producing nanoparticles with a broad diversity of plant metabolites that may aid in the reduction, as well as the different sizes and shapes.

A broad variety of encapsulation techniques has been widened to make nanoparticles dissolve in aqueous medium to offer anchor points where functional molecules can be attached [34,35]. One of the well-known approach to preparing GNPs/GO nanocomposites is to encapsulate GNPs with graphene oxide (GO). GO sheets possessed a mixture of defects,  $\text{sp}^2$  and  $\text{sp}^3$  hybridized carbon atoms. GO sheets contain extraordinary optical properties, due to their capability to adsorb oxygen atoms on their GO surfaces in the form of (-O, -OH, -COOH), and ether functional groups [36]. The above two acid groups like carboxyl and phenol hydroxyl groups are well dispersed in an aqueous medium with

extreme negatively charged surface [37, 38]. For the sensible application of GO, the bioprotection features of GO was studied by several groups [39, 40]. Liao and Akhavan *et al.* have been reported that GO has enriched functional groups, good electrical conductivity, large surface area, good biocompatibility and high stability, which makes it suitable for biomedical applications and sensing of bio-molecules [41-43] such as uric acid, nicotinamide, dopamine, organosulfate pesticides, ascorbic acid, adenine dinucleotide, glucose, cholesterol, protein, histidine and hydrogen peroxide etc. Moreover, GO has exclusive features such as prominent flexibility, facile synthesis, lofty dispersibility in aqueous medium, easily tunable surface functionalization through non-covalent or covalent pathways [44].

In this study, we propose the eco-friendly synthesis of GNPs by using *B. javanica Blume* leaves extract (BJBLE) and GO encapsulated with GNPs for the first time. The formation of GNPs was confirmed by UV-vis spectroscopy, transmission electron microscopy (TEM), X-ray diffraction (XRD), fourier transform infrared spectroscopy (FT-IR) and GO encapsulated GNPs (GO/GNPs) was also confirmed by Scanning electron microscopy (SEM) and EDX spectrum. The GO/GNPs modified GCE demonstrates superior electrochemical detection capability towards dopamine when compared to other modified electrode. The GO/GNPs modified glassy carbon electrode (GCE) exhibits a wide linear range and low limit of detection (LOD) in 0.05 M PBS pH 7. This is the first report, to the best of our knowledge in which green synthesized GNPs derived from BJBLE on the modified GCE employed as an electrochemical sensor for the detection of dopamine.

## 2. EXPERIMENTAL

### 2.1. Materials

The healthy matured *B. javanica Blume* leaves were collected from National Taipei University of Technology, Taipei, Taiwan-106 (Republic of China). The fresh leaves were collected and cleaned with double distilled water (DD). The Chloroauric acid ( $\text{HAuCl}_4 \cdot 3\text{H}_2\text{O}$ ), dopamine and graphite powder was purchased from sigma-Aldrich, Taiwan. All the other chemicals are in the analytical grade and utilized without further purification.

### 2.2. Methods

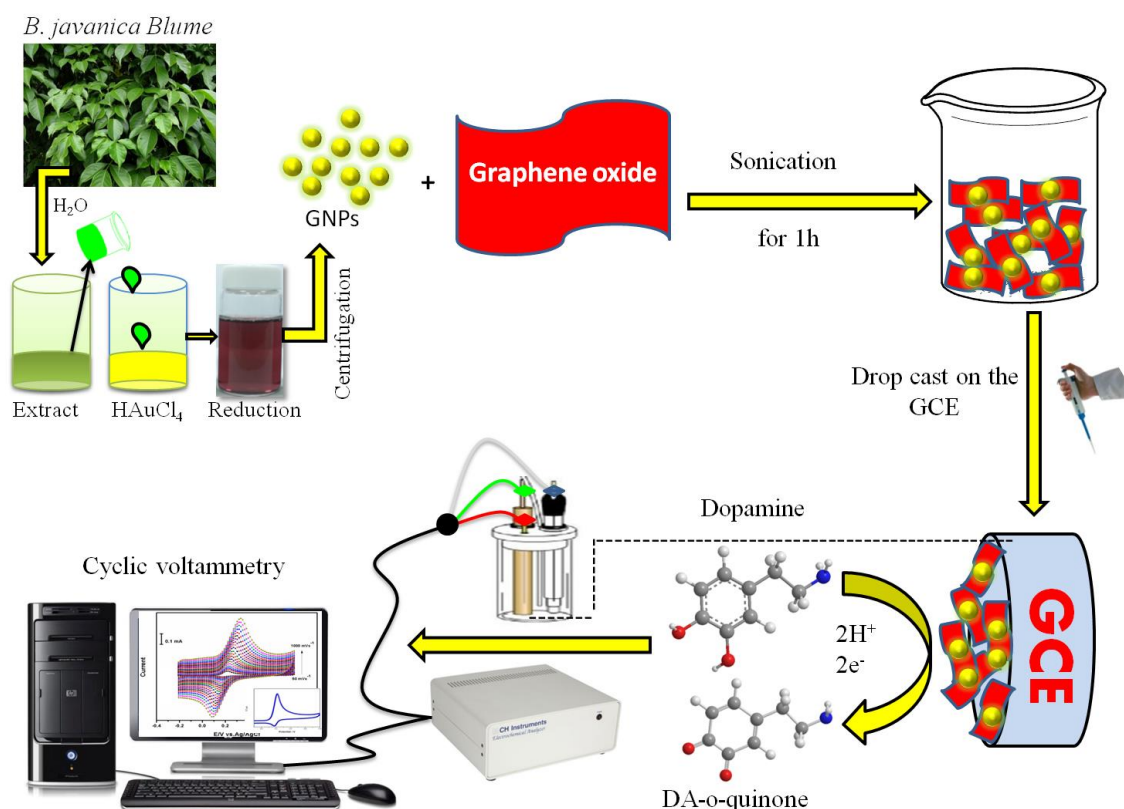
#### 2.2.1. Synthesis of plant extract

First, the collected leaves of *B. javanica Blume* were thoroughly washed with DD water. After that, the leaves were spread over filter paper to remove the wetness of leaf and then dried at room temperature for an hour. Then, the leaves are cut into small fine pieces. 5g of the BJBL were weighed and transferred into 200 mL water in 500 mL beaker and it was boiled in a water bath at 100 °C for 5 min. The mixture was cooled and filtered twice; sequentially the filter liquor was centrifuged at 5000 rpm for 15 min. The aqueous extract (*B. javanica Blume*) obtained then filtered using Whatman filter paper No. 1 and stored at 4 °C for further studies.

### 2.2.2. Green synthesis of GNPs by using the leaf extract

The leaves extract was dried and optimized to 4.5 mL. Further, the optimized extract was mixed with 10.5 mL of 0.5 mM gold solution then the mixer was kept on the table at room temperature, for reduction of  $\text{Au}^{3+}$  to  $\text{Au}^0$ . The formation reaction was very fast as the ruby red color appeared within 10 sec and appearance of ruby red color because of GNPs exhibit surface plasmon resonance (SPR) at 500–550 nm. The formation of GNPs was confirmed by UV-visible spectroscopy analysis in the range of 529 nm. The GNPs obtained were purified by repeated centrifugation at 5000 rpm/min for 15 min and washed several times with DD water. The GNPs were collected and re-dispersed in deionized water for further characterization.

### 2.2.3. Preparation and fabrication of the graphene oxide encapsulated GNPs at modified GCE



**Scheme 1** the schematic view of the synthesis procedure for the preparation of GNPs and GO/GNPs composite and its application for electrochemical sensor dopamine.

Graphite oxide was prepared from raw graphite powder using the modified Hummer's method [45]. After that, the preparation of GO/GNPs by mixing  $2 \text{ mg mL}^{-1}$  of green synthesized GNPs and 2 mL aqueous GO in a beaker. The mixture was allowed to sonication for an hour and the mixture was stored at room temperature for further characterization and electrochemical measurements. The formation of GO/GNPs composite was shown in Fig.4. Above GO/GNPs composites  $8 \mu\text{L}$  (optimized concentration) was drop casted on the polished GCE surface and it's allowed to dry at room

temperature. After that, the dried GO/GNPs/GCE washed smoothly with DD water to remove loosely bounded composites. Then this electrode allowed to do further electrochemical measurements. The overall procedures for the preparation and fabrication of the GNPs and composite are shown in scheme 1.

#### 2.2.4. Characterization of GNPs and GO/GNPs composites

UV-visible spectral analysis of *B. javanica Blume* was performed in a Jasco V-770 UV-visible spectrophotometer. The absorption maxima were analyzed in the 400–800 nm wavelength range at different time intervals. The powder XRD were analyzed as- prepared green synthesized GNPs in XPERT-PRO (PANalytical B.V., The Netherlands) diffractometer (Cu K $\alpha$  radiation,  $k$  1/4 1.54 Å). FTIR analysis was recorded by using a Thermo Nicolet Nexus 670 spectrometer in the range of 4000–400  $\text{cm}^{-1}$  to determine the presence *B. javanica Blume* derived bioactive compounds in BJBLE GNPs. The chemical constituents of plant leaves extract was identified before and after addition of gold solution through the gas chromatography- mass spectroscopy (GC-MS) (HP 6890GC/5973MS, Agilent Technology, Little Falls, California, USA) instrument. The size and shape of the particles were measured with HR-TEM using JEOL 3010 equipped with selected area electron diffraction pattern (SAED). The GO/GNPs composites were confirmed by scanning electron microscopy attached with elemental analysis (SEM- Hitachi S-3000 H). All the electrochemical studies were performed in CHI 405a and CHI 900 electrochemical analyzer (CH Instruments, USA). The conventional three electrode system has been employed for the electrochemical measurements where GCE (area 0.071  $\text{cm}^2$  & rotating disc carbon electrode (RDCE) = 0.2  $\text{cm}^2$ ) used as a working electrode, platinum wire as a counter electrode and saturated silver/silver chloride (Ag/AgCl) electrode as a reference electrode. All the electrochemical studies have been carried out in 0.05 M PBS.

### 3. RESULTS AND DISCUSSION

#### 3.1. UV-vis spectral analysis

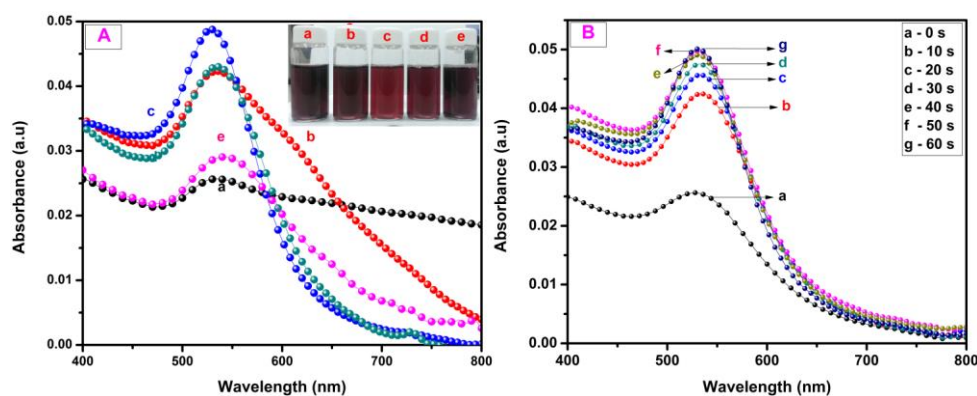


**Figure. 1** UV-vis spectra of green synthesized GNPs (A) Effect of the plant concentration (a) 12.5 mL of 0.5 mM gold solution and 2.5 mL of BJBLE (b) 11.5 and 3.5 mL (c) 10.5 and 4.5 mL (d) 9.5 and 5.5 mL (e) 8.5 and 6.5 mL respectively. (B) UV-visible spectra of the reaction mixture at different time intervals at room temperature (a-g; 0 to 60 sec).

UV-vis spectroscopy is a very significant phenomenon to validate the stability, shape and size of the MNPs in an aqueous solution. In order to investigate the shape and size of the GNPs was initially monitored by UV-vis analysis. A different concentration of BJBLE and gold solutions are represented in Fig.1A. The extract concentration was increased and the gold solution concentration was decreased from (a) 12.5 mL of 0.5 mM gold solution and 2.5 mL of BJBLE, (b) 11.5 and 3.5 mL (c) 10.5 and 4.5 mL, (d) 9.5 and 5.5 mL, (e) 8.5 and 6.5 mL respectively. The inset figure shows the digital photograph of formation of GNPs (different concentration of BJBLE and gold solution) with corresponding to the absorption spectra. The color changes from dark pink (a, b) to ruby red (c), and the concentration of BJBLE (d, e) again increased a dark pink color was formed corresponding to the absorption spectrum as shown in Fig.1A. The change of GNPs color depends on the volume of BJBLE and gold solution. The GNPs functionalized with BJBLE gave uniform sharp peaks with varying intensities. The 10.5 ml 0.5 mM gold solution and 4.5 mL plant extract gave a uniform and sharp SPR (Surface Plasmon Resonance) band peak at 529 nm, with this ratio a bulk solution was made for further studies.

In order to study the stability and formation of the prepared GNPs in the colloidal solution were investigated by UV-vis analysis. Fig.1B reveals the UV-vis spectrum of gold colloids with various time intervals at 0, 10, 20, 30, 40, 50, 60 sec. the optimized concentration of gold and plant extract mixed solution was taken for the stability studies. From the Fig.1B, which is clearly observed that the bioreduction of gold ions to GNPs started within 0 sec and increasing the time intervals (from 0 to 60 sec) the GNPs formation was reached a saturated level within 40 sec. this results suggested that the biosynthesis of GNPs was very rapid formation. The maximum absorbance for GNPs was monitored at 529 nm, and it look like a little broad spectrum, suggesting their polydispersed nature.

### 3.2. Characterization of the green synthesized GNPs

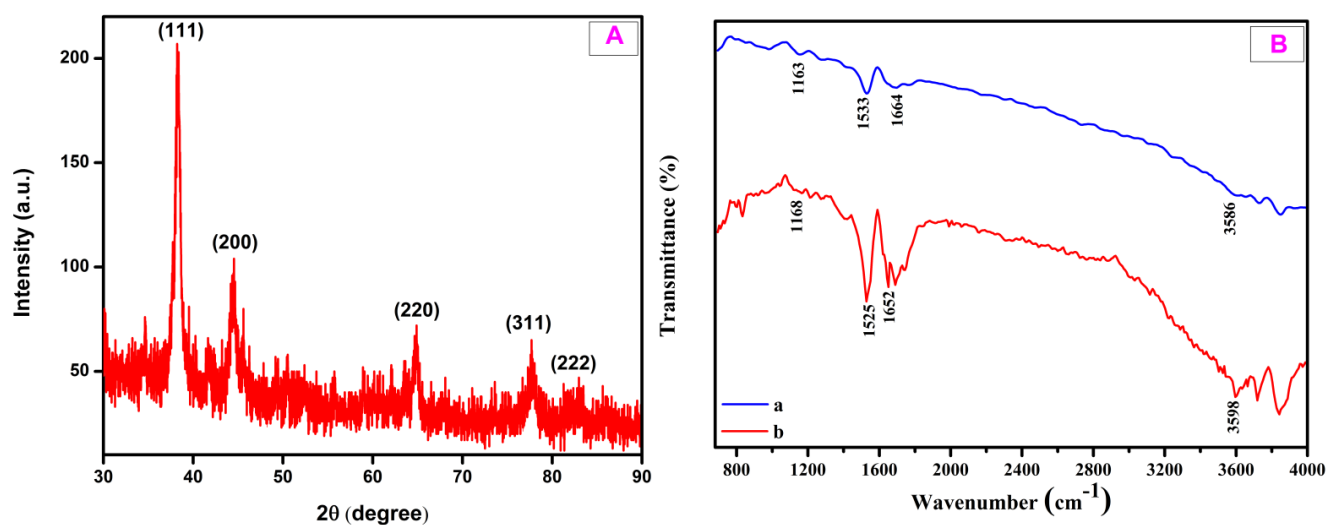


**Figure 2.** Green synthesized GNPs (A) X-ray diffraction pattern (B) FTIR spectra of *B. javanica* Blume extract (a) synthesized GNPs (b).

The phase and crystallographic structure of the synthesized GNPs were studied by XRD. The XRD patterns of as synthesized GNPs as shown in Fig.2A. The peaks at the  $2\theta$  angles of  $38.35^\circ$ ,  $44.55^\circ$ ,  $64.82^\circ$ ,  $77.76^\circ$  and  $81.70^\circ$  were corresponding to (111), (200), (220), (311) and (222) planes of face-centered cubic (fcc) phase of gold [JCPDS File No. 04-0784] [46,47]. The remaining diffraction peaks may be the other phytochemical compounds present in BJBLE and the result suggested that GNPs are highly pure.

$$X_s = \frac{k\lambda}{\beta \cos\theta} \quad (1)$$

Where  $X_s$  is the size of crystalline,  $\lambda$  is the wavelength of X-ray radiation,  $\beta$  is the full width at half maximum (FWHM) of the diffraction peak,  $\theta$  is diffraction angle and  $k$  is Scherer's constant. The average size of crystalline GNPs was calculated from the (111) plane using standard Scherer's formula [48]. The average crystalline size of GNPs was calculated as approximately 29.4 nm size which is in good agreement with HR-TEM results.

FTIR analysis was used for the characterization of the leaf extract and the synthesized GNPs nanoparticles as shown in Fig.2B. The FTIR spectra of leaf extract before and after reduction have shown considerable changes. FT-IR spectra were carried out to discover the organic biomolecules BJBLE responsible for the reduction of GNPs. The sharp peak at  $1533\text{ cm}^{-1}$  was assigned to the  $\text{-N-H}$  stretching vibration of the amide function group [49]. After the bioreduction GNPs, the intensities of peak become sharper from  $1533$  to  $1525\text{ cm}^{-1}$ . Furthermore, a small shift from  $1664\text{ cm}^{-1}$  to  $1652\text{ cm}^{-1}$  was attributed to  $\text{C=O}$  stretching vibration of the carbonyl and ketones groups [50-52]. The peak around at  $1163\text{ cm}^{-1}$  corresponds to  $\text{C-O}$  stretching vibration of alcohols, carboxylic acids, esters and ethers. The peak observed at  $3586\text{ cm}^{-1}$  was relevant to  $\text{O-H}$  stretching vibration. This result indicates the presence of hydroxyl, carboxylic acids, esters, ethers and carbonyl groups in BJBLE which may be accountable for the reduction of the Au ions and stabilization of Au nanoparticles.

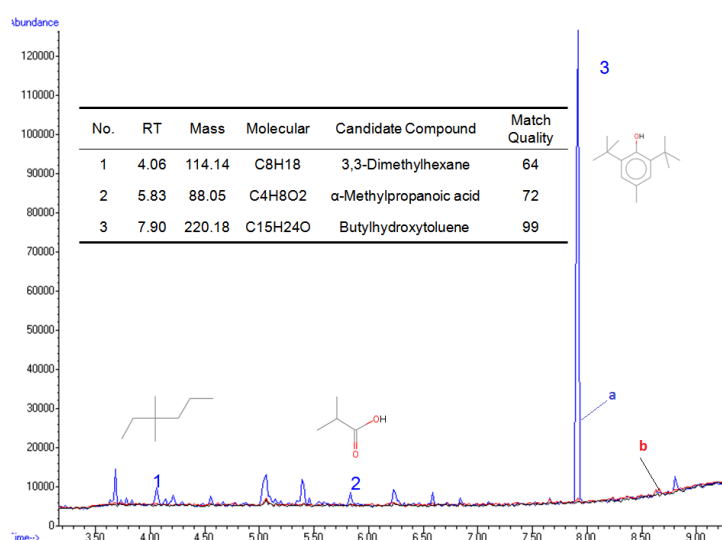


**Figure 3.** GC-MS chromatograph of BJBLE leaves extract (a) and after reduction of GNPs (b).



Phytochemical constituents present in the BJBLE which was identified through GC-MS. GC-MS chromatograph of leaf extract showed three major peaks, each peak indicating the presence of three chemical compounds. Their chemical structure, chemical formula, molecular weight, peak area (%), retention time are presented in inserted Fig.3. Fig.3 (a) shows the only pure plant extract and Fig.3 (b) shows the after reduction GNPs. The major compounds present in BJBLE such as 3,3-Dimethylhexane,  $\alpha$ -Methylpropanoic acid, Butylhydroxytoluene (BHT). The BJBLE of BHT is a most commonly used antioxidant. This BHT compound may play a vital role in the reduction process of  $\text{Au}^{3+}$  to  $\text{Au}^0$ . The leaf extract of *B. javanica* Blume can also be used as a potential source for the isolation of those compounds.

### 3.3. TEM analysis

The morphology and structure evolution of the GNPs were observed by HR-TEM as shown in Fig.4. The TEM images (Fig. 4 A, B) of GNPs showed that spherical like morphology nanoparticles and their sizes from 20 to 10 nm. The very slight agglomeration was occurred, which may be possible sedimentation at the latter stage of the reaction. Fig.4C shows the High resolution TEM was carried out to further observe the GNPs. It showed that the lattice fringes was  $d=0.234$  nm, which was coincidental with the theoretical spacing for (111) plane of the GNPs.

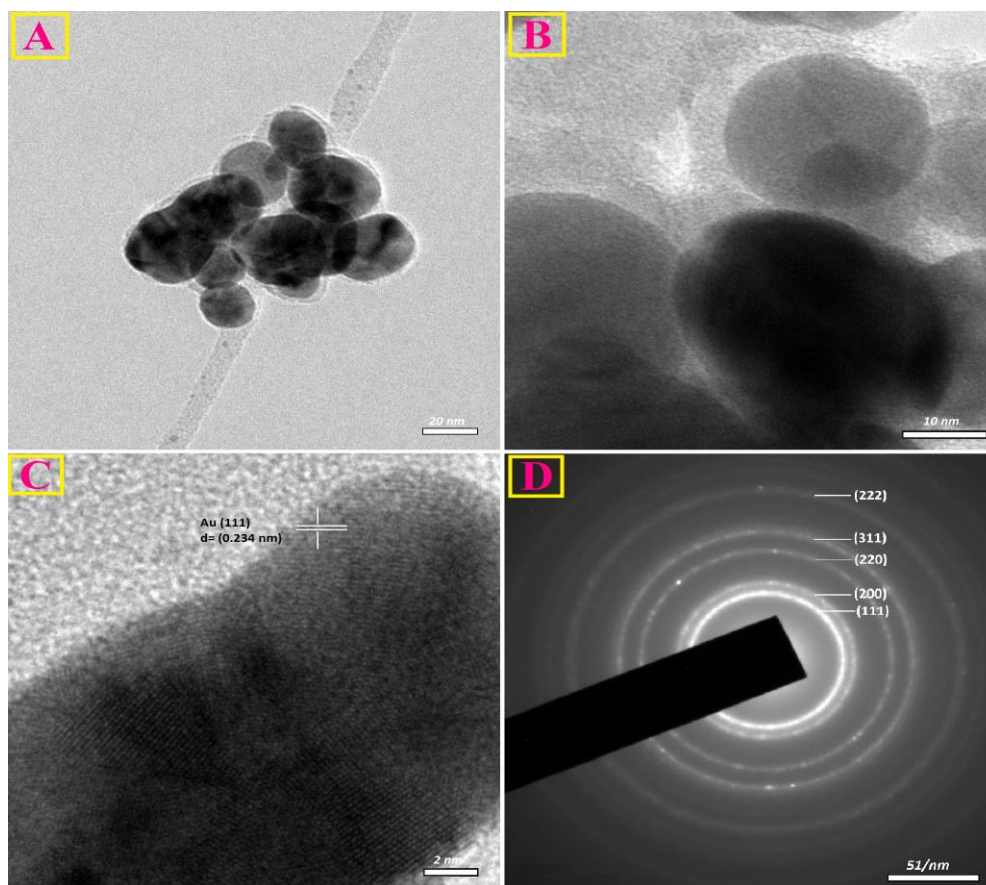


**Figure 4.** HRTEM images of as-synthesized GNPs at different magnification (A) 20 nm (B) 10 nm (C) Lattice fringes (D) SAED pattern of GNPs.



The SAED pattern for GNPs and the ring pattern are indexed to the 111, 200, 220, 311 and 222 Bragg reflections from the fcc phase of gold as revealed in Fig.4D. The crystalline natures of the GNPs clear from the SAED pattern. It is also found that the single crystalline nature and it was determined by SAED pattern which was in accordance with XRD result.

### 3.4. Graphene oxide encapsulated green synthesized GNPs

The morphology of the GO/GNPs composites were investigated by SEM. Fig.5 shows the SEM images of GO (A) and encapsulated GNPs on the GO sheet (B) and corresponding to the EDX spectrum of GO (C) GO/GNPs composites (D). It could be clearly seen that the GO sheet exhibited a typical rippled morphology with bulk paper like layers and then introduced green synthesized GNPs into the GO solution; electrostatic interaction takes place between GNPs and GO [53]. Furthermore, the electrostatic interaction between GO and GNPs, which upon mixing, allowing the GO encapsulated GNPs formed and it was clearly shown in Fig.5 (B).

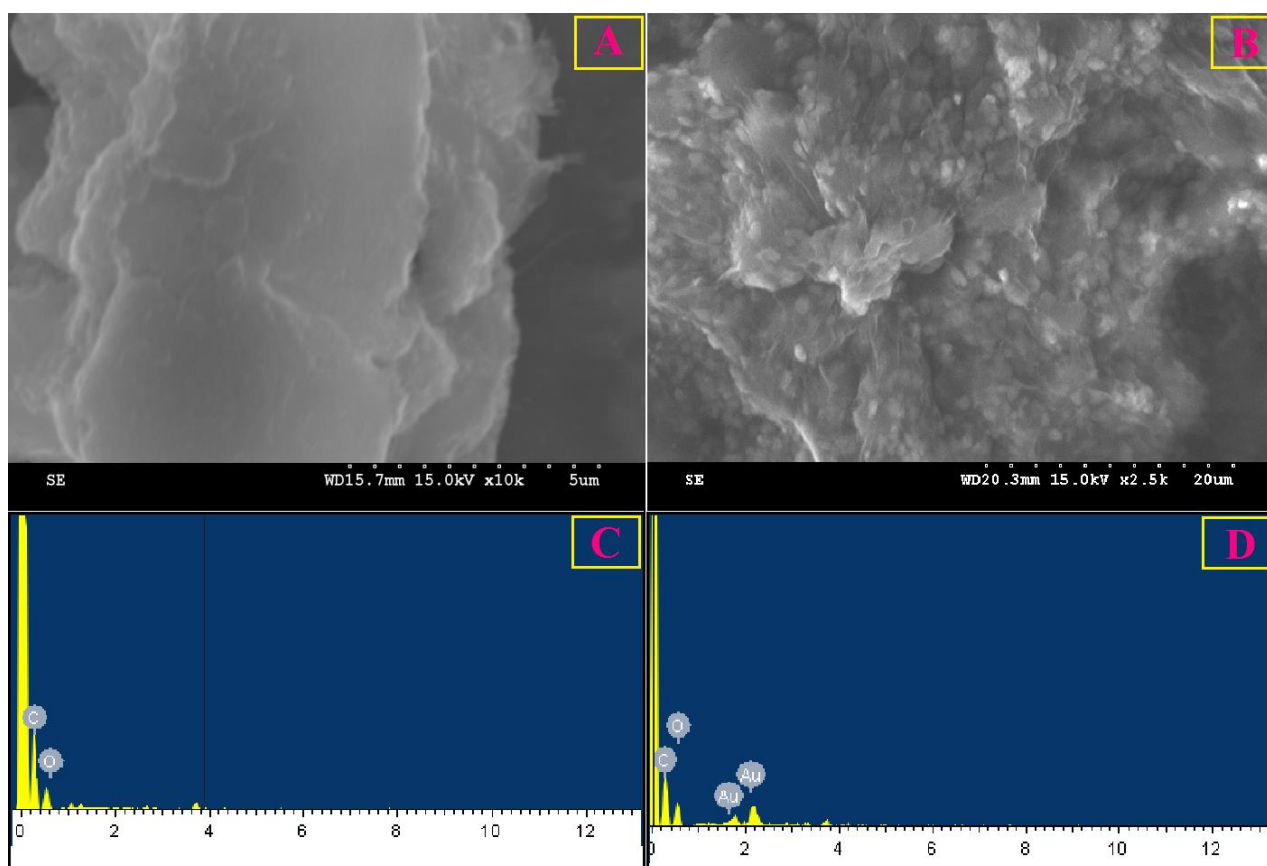


**Figure 5.** SEM images (A) GO (B) GO encapsulated green synthesized GNPs (C and D) Corresponding to the EDX spectrum of GO and GO/GNPs composites.

The merits of the proposed approach are that it can be performed at room temperature and that the size and structure of the nanoparticles used remains unchanged after encapsulation and also it was

confirmed by EDX. Fig.5 (C and D) illustrates the energy dispersive EDX spectrum of GO and GO/GNPs composite. From the EDX results, it is clear that the presence of carbon and oxygen elements in GO and Au, carbon and oxygen in GO/GNPs composite respectively. The above result suggests GO encapsulated green synthesized GNPs, which make them very excellent modified electrode material for the electrochemical detection of dopamine sensor.

### 3.5. Electrochemical performance of dopamine at various modified electrodes

The electrochemical performance of dopamine was examined at various modified electrodes by using CVs in presence of 300  $\mu\text{M}$  dopamine. Fig.6 depicts the CVs response in absence of dopamine (a) bare GCE, (b) GO/GNPs/GCE, and the presence of 300  $\mu\text{M}$  of dopamine (c) GO/GNPs/GCE, (d) bare GCE, (e) GNPs/GCE, (f) GO/GCE containing 0.05M phosphate buffer solution (PBS pH 7) at a scan rate of 50  $\text{mV s}^{-1}$ .

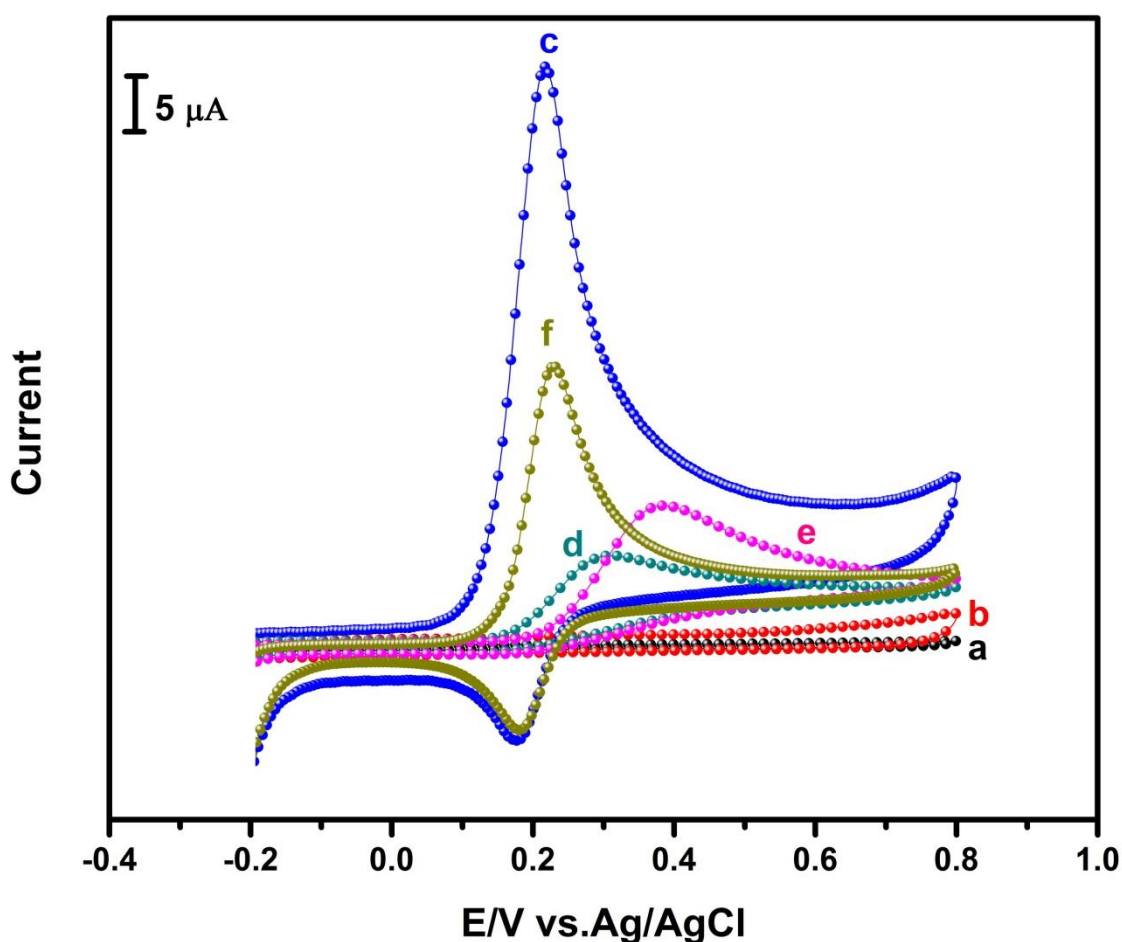


**Figure 6.** Cyclic voltammetry performance of absence of dopamine (a) bare (b) GO-GNPs, and presence of (c) GO/GNPs/GCE (d) bare GCE (e) GNPs/GCE (f) GO modified GCE in 0.05M PBS containing 300  $\mu\text{M}$  of dopamine at a scan rate of 50  $\text{mV s}^{-1}$

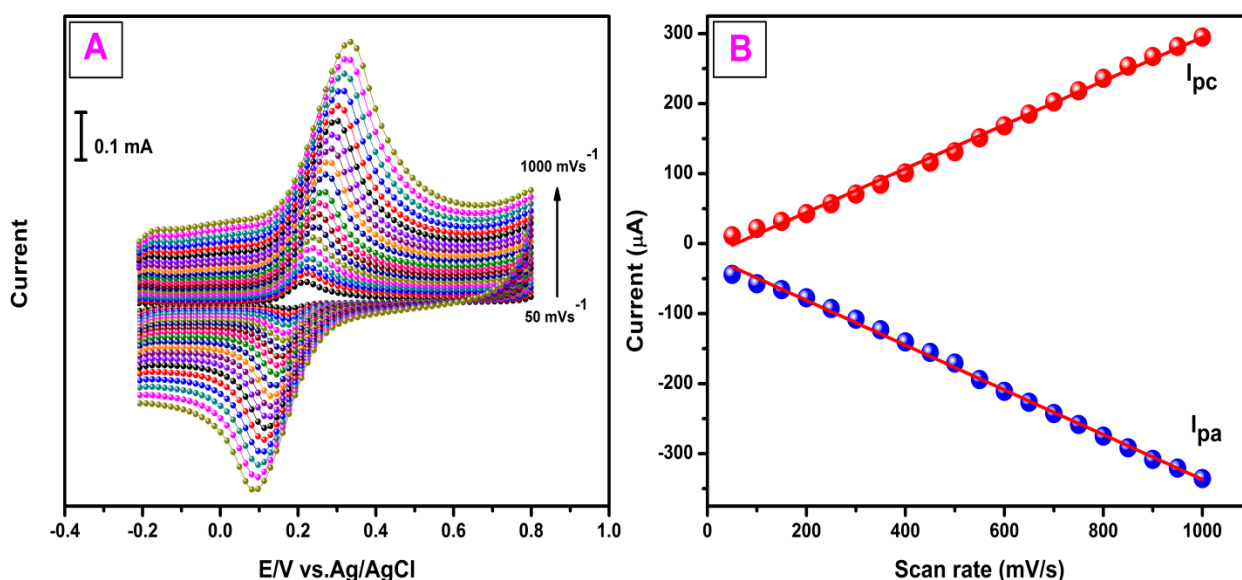


**Figure 7.** (A) Cyclic voltammograms of 300  $\mu\text{M}$  dopamine at GNPs/GO/GCE in 0.05M PBS (PH 7) at different scan rates (inside to outside; 50–1000  $\text{mVs}^{-1}$ ) (B) The plot between scan rate vs. peak currents

A broad irreversible oxidation peak of dopamine was identified at 0.311V in bare GCE. The GNPs/GCE and GO/GCE demonstrated a couple of quasi-reversible redox peaks for dopamine at the reduction peak potential ( $E_{pc}$ ) and oxidation peak potential ( $E_{pa}$ ) of 0.170 and 0.386 V, 0.181 and 0.229 V respectively. The peak to peak separation for GNPs/GCE and GO/GCE in dopamine was found as 216 and 48mV respectively. While the GO/GNPs modified GCE in the presence of dopamine revealed a pair of very sharp and well-defined quasi-reversible redox peaks at 0.174 ( $E_{pc}$ ) and 0.218 V ( $E_{pa}$ ). The peak to peak separation was established as 44 mV. The oxidation peak current of dopamine at GO/GNPs modified GCE was 4.32 and 2.01 fold higher than that of other modified GCE such as GNPs/GCE and GO/GCE. In addition, the dopamine oxidation overpotential of GO/GNPs at modified GCE was 168 and 11 mV lower compare than other GNPs and GO modified electrodes. The above results suggesting that the modified GO/GNPs GCE is very promising and active electrode material for detection of dopamine. Furthermore, the good communication ability of green synthesized GNPs with GO resulting in the increased electrochemical performance and lesser oxidation potential for the recognition of dopamine.

Fig.7A and B illustrates the CVs of GO encapsulated green synthesized GNPs composites modified GCE in a nitrogen atmosphere (deoxygenated) PBS (pH 7) containing 300  $\mu\text{M}$  of dopamine at different scan rates. Upon increasing the scan rates from 50 to 1000  $\text{mVs}^{-1}$ , the cathodic ( $I_{pc}$ ) and anodic peak ( $I_{pa}$ ) currents increased and both redox peak potential ( $E_p$ ) was slightly shifted. The anodic peak current shifted towards positive side and the cathodic peak current shifted towards negative side at higher scan rates. The anodic and cathodic peak currents have a linear dependence (Fig.7B) against the scan rates vs  $I_p$ , suggesting that the dopamine oxidation process at the green synthesized GO/GNPs composites at modified electrodes is a surface controlled not diffusion controlled process [54].

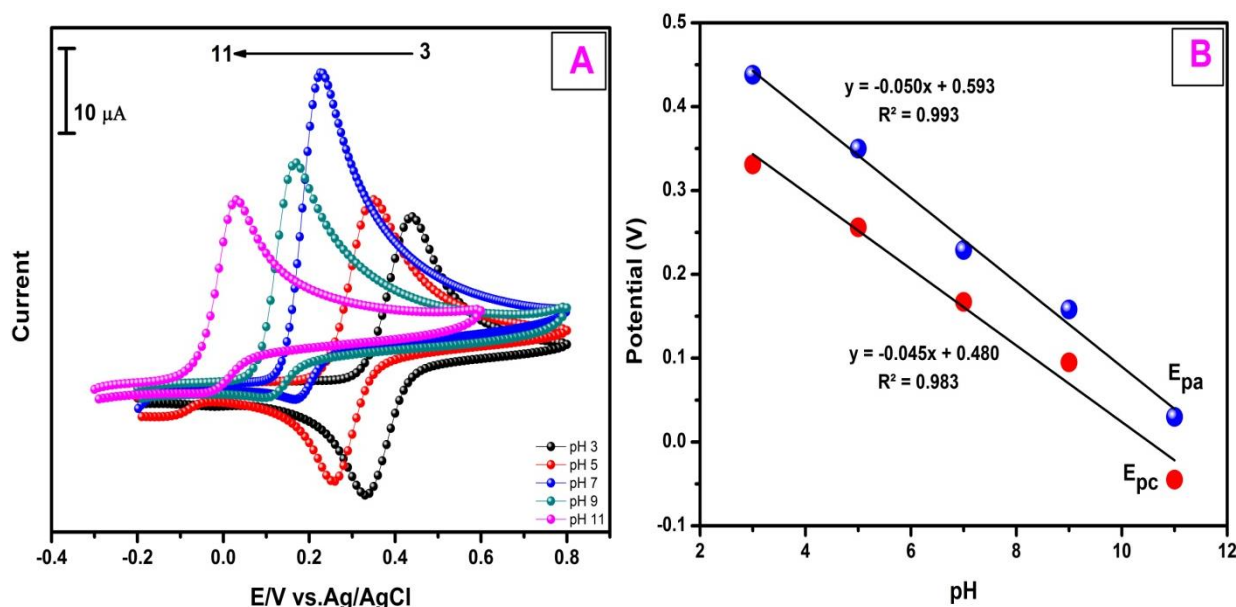
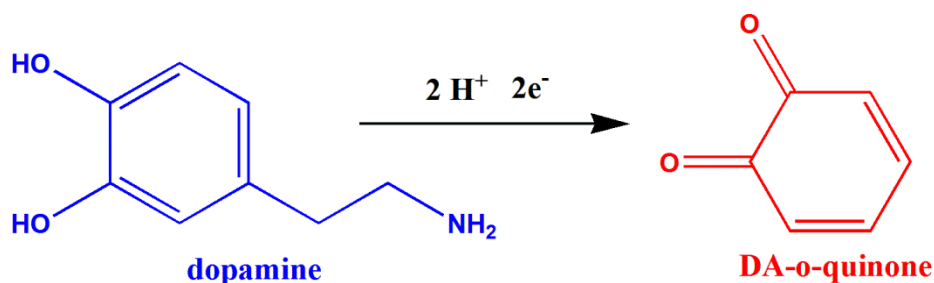


**Figure 8.** (A) Cyclic voltammetry response of GO/GNPs composite modified GCE for 300  $\mu\text{M}$  of dopamine containing various pH solutions (pH 3 to 11) at a scan rate of 50  $\text{mV s}^{-1}$ . (B) Calibration plot for  $E_p$  vs. pH.



**Scheme 2.** Oxidation mechanism of dopamine

The effect of pH played a major role in the dopamine oxidation process at the GO/GNPs composites modified GCE, so we examined the various pH in  $\text{N}_2$  saturated PBS solution in the presence of 300  $\mu\text{M}$  dopamine at the scan rate of 50  $\text{mVs}^{-1}$  by CVs. Fig.8A reveals the CVs signals of GO/GNPs modified GCE for 300  $\mu\text{M}$  of dopamine containing various pH solution 3 to 11 (right to left in Fig.8A). At the composite electrode both the cathodic and anodic peak potential shifted towards negative direction upon increasing the pH range from 3 to 11 and the peak current also increased upto 3 to 7, then again increase the pH range (above pH 7) the peak current was decreased. The maximum current was achieved at pH 7 compared to other pH solution. So we have chosen pH 7 for further electrochemical measurements. This result suggests that the oxidation process of dopamine in modified GCE is pH dependent reaction. Fig.8B shows the calibration plot of different pH vs. different peak potential, the slope value was observed to be  $E_{pa}$  (V) -0.050 V/pH using regression equation. According to the Nernst equation, the calculated slope value  $E_{pa}$  -50 mV/pH was very closed to the theoretical value of -59 mV/pH for an equal number of electron and proton transferred in electrochemical reaction [55]. The result further validates that the electrochemical redox reaction of

dopamine at the GO/GNPs composite modified GCE is two protons ( $2\text{H}^+$ ) and two electrons ( $2\text{e}^-$ ) transferred electrochemical process as shown in scheme 2.

### 3.6. Calibration curve studies

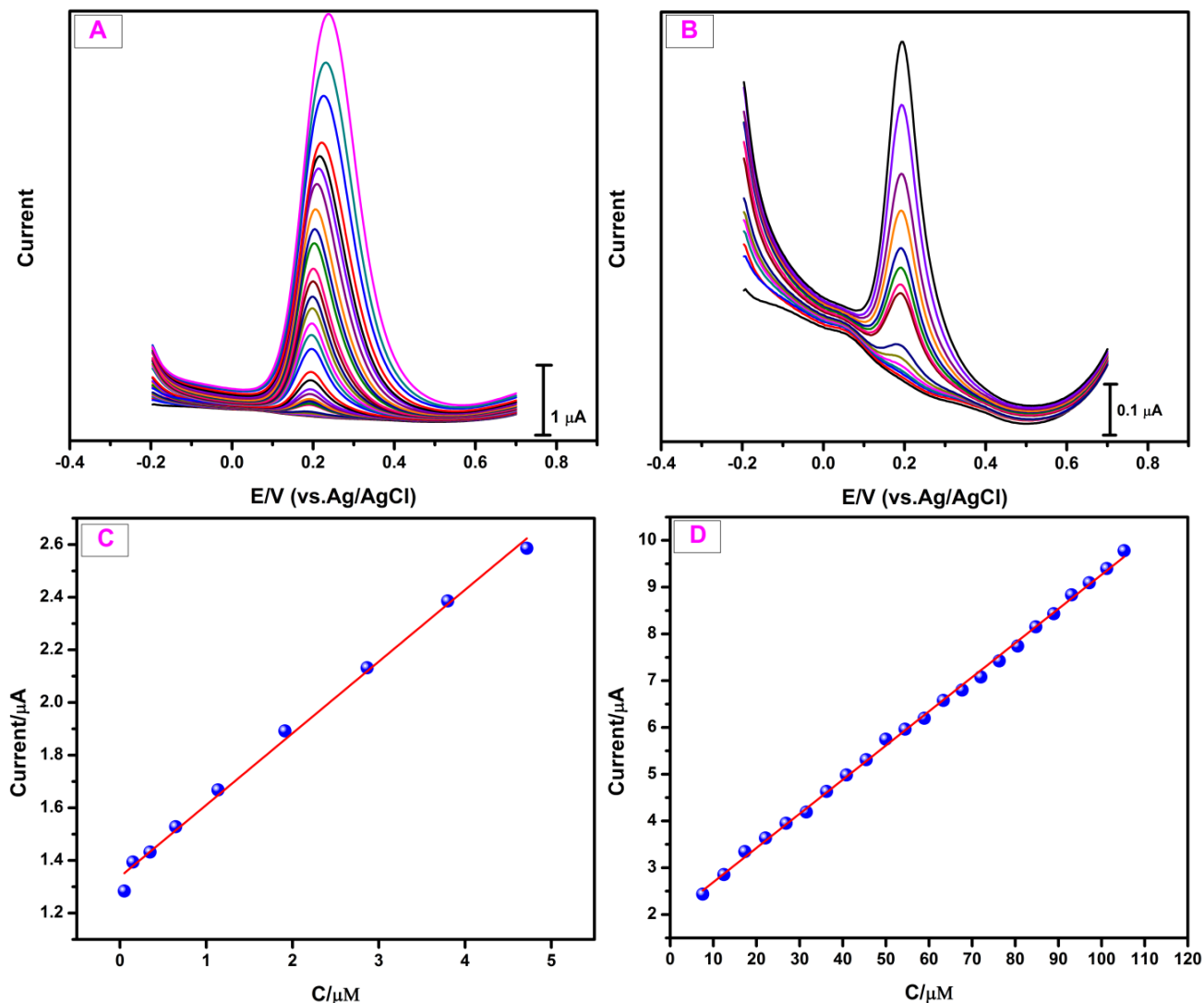


**Figure 9.** (A) DPV response of GO/GNPs modified GCE with increasing the concentration of dopamine from 0.049 to 105  $\mu\text{M}$ . (B) Lower concentration of dopamine ranges from 0.049 to 28.5  $\mu\text{M}$  (C) The calibration Plot of oxidative current vs. dopamine concentration (lower) (D) The calibration Plot of oxidative current vs. dopamine concentration (higher).

Difference pulse voltammetry (DPV) is an important electrochemical technique to quantitative analysis of dopamine and also DPV has a greatly higher current sensitivity and enhanced resolution compared to CVs and other electrochemical techniques. Fig.9 shows the GO/GNPs at modified GCE to successive addition of dopamine with concentration from 0.049 to 105  $\mu\text{M}$  in 0.05 M PBS (pH 7). Fig.9A reveals a very sharp and well defined anodic peak current observed at peak potential 0.18V, a further increase in the concentration of dopamine the anodic peak current was also increased and finally reached a level. Fig.9B shows the lowest concentration of dopamine range from 0.049 to 28.5

$\mu\text{M}$  and observed well sharp anodic peaks it does suggest that the sensitivity is very high towards oxidation of dopamine at GO/GNPs modified GCE. Two linear ranges observed from the Fig.9A by DPV, Fig.8C is first linear range was obtained 0.049 to 4.7  $\mu\text{M}$  with the linear equation of  $I(A) = y = 0.272x + 1.138$ , ( $R^2 = 0.995$ ) with sensitivity  $3.443 \mu\text{A}\mu\text{M}^{-1}\text{cm}^{-2}$ . The calculated detection limit was 0.03  $\mu\text{M}$ . Fig.8D is second linear range was 7.5–105  $\mu\text{M}$  with the linear equation of  $I(A) = y = 0.073x + 1.962$ , ( $R^2 = 0.998$ ) and the sensitivity of  $0.911 \mu\text{A}\mu\text{M}^{-1}\text{cm}^{-2}$ . However, the good linear response was still obtained, and results showed that the GO encapsulated green synthesized GNPs at modified GCE exhibited an improved performance when compared with previous literature as it can be summarized in Table 1.

**Table 1.** Comparison on the efficiency of modified electrodes for the determination of dopamine

Modified Electrode	Linear range ( $\mu\text{M}$ )	LOD ( $\mu\text{M}$ )	Ref
PEI/[( $\text{P}_2\text{W}_{17}\text{V}-\text{CuO}$ )/(CS Pd)] <sub>7</sub> /( $\text{P}_2\text{W}_{17}\text{V}-\text{CuO}$ /ITO) <sup>a</sup>	0.25–217	0.045	56
MWCNTs/Nafion/ITO	0.01-10	0.2	57
GO/GCE	1-15	0.27	58
PI <sub>max</sub> -GO/GCE	12-278	0.63	59
RGO/Pd-NPs/GCE	1-150	0.233	60
GP-MWCNTs-AuNCs/GCE	2-213	0.67	61
Graphene/chitosan/GCE	0.1-140	0.05	62
Graphite nanosheet/nafion	0.5-10	0.2	63
Au-NPs/polyaniline	3 - 115	0.8	64
Dopamine grafted ERG/PMB/GCE	0.96-7.68	1.03	65
GO/GNPs/GCE	0.049 - 4.7 7.5–105	0.03	This work

<sup>a</sup>vanadium-substituted polyoxometalate, CuO and Pd nanoparticles; ITO- Indium tin oxide; GO- Graphene oxide; GCE- Glassy carbon electrode; PI<sub>max</sub>-polyimidazole; RGO/Pd-NPs- Reduced graphene oxide/ palladium nanoparticles; GP-MWCNTs-AuNCs- Graphene-Multiwall Carbon Nanotube-Gold Nanocluster; Au-NPs- Gold nanoparticles; ERG/PMB -dopamine grafted graphene oxide/poly(methylene blue); GNPs- Gold nanoparticles.

### 3.7. Anti-interference and stability studies

Selectivity is very important to study the electrochemical biosensor, in order to investigate the selectivity of the fabricated dopamine sensor, effect of some biological interferents are very close oxidation potential to the dopamine sensor such as AA (b), UA (c) and glucose (d) have been studied.



Fig.10. reveals the amperometric ( $i-t$ ) curve at the applied potential of 0.2V using GO/GNPs modified RDCE.

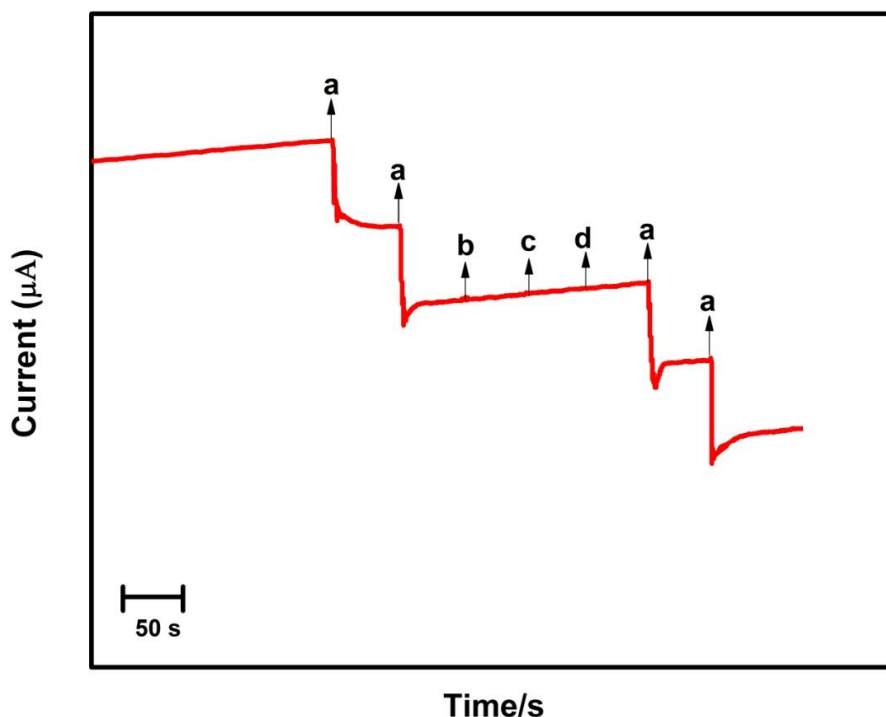


**Figure 10.** Effect of interfering species on the biosensor response with subsequent addition of 20 fold excess of dopamine (a) ascorbic acid (b) uric acid (c) glucose (d) in the 0.05 M PBS (pH 7).

From the results a well-defined current response was observed in the addition of 100  $\mu\text{M}$  dopamine (a) and biologically co-interfering compounds (b), (c) and (d) could not show any significant response in addition of 20 fold excess of those biological compounds, indicating that the fabricated GO/GNPs modified RDCE is highly selective towards the determination of dopamine. The electrode stability is a very important factor for all innovatively developed electrochemical sensors. The oxidation peak current response of 100  $\mu\text{M}$  dopamine at GO/GNPs composite modified electrode was studied for 7 days and stored in PBS when not in use. The GO/GNPs modified electrode retained 93.6 % of its initial current response after 7 days, which suggests the good storage stability of the sensor.

### 3.8. Real sample analysis

To study the practicability of GO/GNPs modified GCE dopamine sensor, the determination of dopamine in real biological samples was evaluated. Thus, the GO/GNPs/GCE was applied to the detection of dopamine in biological fluids such as human blood serum and urine by amperometry. The collected serum and urine samples were four times diluted by 0.05M PBS (pH 7) and it was directly used for the detection of dopamine. The amperometric response of dopamine oxidation was consecutively recorded for the addition of blood serum and urine samples, followed by the addition of 0.01M dopamine by different time interval. The obtained recoveries of dopamine were given in Table 2. The GO/GNPs/GCE dopamine sensor achieved noteworthy recovery results from 96.2 to 103 %.

Therefore, the developed GO/GNPs/GCE dopamine sensor was applicable for the practical applications.

**Table 2.** Determination of dopamine in biological samples by using GO/GNPs/GCE

Real sample	Add ( $\mu\text{M}$ )	Found <sup>a</sup> ( $\mu\text{M}$ )	Recovery (%)
Blood serum	5	4.81	96.2
	10	9.9	99
Urine	5	5.1	102
	10	10.3	103

<sup>a</sup>Standard deviation method and <sup>b</sup>Relative standard deviation with three repetitive measurements.

#### 4. CONCLUSION

In concise, GO encapsulated green synthesized GNPs were effectively synthesized *via* a simple, green approach and are cost effective. A sensitive electrochemical sensor with GO encapsulated green synthesized GNPs was developed for the determination of dopamine and the composite modified electrode showed significantly improved peak current towards the oxidation of dopamine. The GO/GNPs based electrochemical sensor exhibited electron transfer rate and excellent electrocatalytic activity towards the oxidation of dopamine. In addition, the modified electrode demonstrated good sensitivity and low detection limit ( $0.03\mu\text{M}$ ) in the detection of DA and good selectivity towards the biological interferences AA, UA and glucose. These results exposed GO/GNPs/GCE could be a good potential candidate for electrochemical sensor application of dopamine.

#### ACKNOWLEDGMENT

The authors gratefully acknowledge the financial support of the Ministry of Science and Technology, Taiwan through contract nos. NSC101-2113-M-027-001-MY3 to S.M Chen. The financial support from the Chung Gung Memorial Hospital through contract no. BMRP 280 to B.S. Lou is also acknowledged.

#### References

1. J. Bergquist, A. Sciubisz, A. Kaczor, J. Silberring, *J. Neurosci. Methods*, 113 (2002) 1-13.
2. A.S. Adekunle, B.O. Agboola, J. Pillay, K.I. Ozoemena, *Sensors & Actuators B:Chemical*. 148 (2010) 93–102.
3. S. Komathi, A.I. Gopalan, K.P. Lee, *Analyst*. 135 (2010) 397–404.
4. Z. Seckin, M. Volkan, *Anal. Chim. Acta*, 547 (2005) 104-108.
5. H. Wang, Q. Hui, L. Xu, J. Jiang, Y. Sun, *Anal. Chim. Acta*, 497 (2003) 93-99.
6. C. Muzzi, E. Bertocci, L. Terzuoli, B. Porcilli, I. Ciari, R. Pagani, R. Guerranti, *Pharmacother*, 62 (2008) 253-258.
7. M.A. Fotopoulou, P.C. Ioannou, *Anal. Chim. Acta*, 462 (2002) 179-185.

8. K. Jackowska, P. Kryszynski, *Anal. Bioanal. Chem*, 405 (2013) 3753–3771.
9. C.R. Raj, T. Okajima, T.J. Ohsaka, *Electroanal. Chem*, 543 (2003) 127–133.
10. J.F. Cabrita, L.M. Abrantes, A.S. Viana, *Electrochim. Acta*, 50 (2005) 2117–2124.
11. H. Zhao, Y.Z. Zhang, Z.B. Yuan, *Electroanalysis*, 14 (2002) 1031–1034.
12. M.E. Snowden, P.R. Unwin, J.V. Macpherson, *Electrochem. Commun.* 13 (2011) 186–189.
13. S. Ku, S. Palanisamy, S.M. Chen, *J. Colloid Interface Sci*, 411 (2013) 182–186.
14. A. Ciszewski, G. Milczarek, *Anal. Chem*, 71 (1999) 1055–1061.
15. G.Y. Jin, Y.Z. Zhang, W.X. Cheng, *Sensors & Actuators B:Chemical*, 107 (2005) 528–534.
16. W.E. Zhang, B. Xu, L.C. Jiang, *J. Mater. Chem*, 20 (2010) 6383–6391.
17. P. Si, H. Chen, P. Kannan, D.H. Kim, *Analyst*, 136 (2011) 5134–5138.
18. L. Wu, L. Feng, J. Ren, X. Qu, *Biosens. Bioelectron*, 34 (2012) 57–62.
19. K. Yokohama, D.R. Welchons, *Nanotechnology*, 18 (2007) 105101–105107.
20. N. Roy, A. Gaur, A. Jain, S. Bhattacharya, V. Rani, *Environ. Toxicol. Phar*, 36 (2013) 807–812.
21. V.V. Makarov, A.J. Love, O.V. Sinitsyna, S.S. Makarova, I.V. Yaminsky, M.E. Taliany, N.O. Kalinina, *Acta Naturae*. 6 (2014) 35–44.
22. R. Karthik, Shen-Ming Chen, A. Elangovan, P. Muthukrishnan, R. Shanmugam, Bih-Show Lou, *J. Colloid Interface Sci*, 468 (2016) 163–175.
23. R. Karthik, R. Sasikumar, Shen-Ming Chen, M. Govindasamy, J. Vinoth Kumar, V. Muthuraj, *Int. J. Electrochem. Sci.*, 11 (2016) 8245 – 8255.
24. R. Karthik, Yu-Shen Hou, Shen-Ming Chen, A. Elangovan, M. Ganesan, P. Muthukrishnan, *J IND ENG CHEM*, 37 (2016) 330–339.
25. M. Hu, J. Chen, Z. Y. Li, L. Au, G. V. Hartland, *Chem. Soc. Rev*, 35 (2006) 1084–1094.
26. R. Karthik, M. Govindasamy, S.M. Chen, V. Mani, Bih-Show Lou, R. Devasenathipathy, Y.S. Hou, A. Elangovan, *J. Colloid Interface Sci*, 475 (2016) 46–56.
27. C.H. Ramamurthy, M. Padma, I.D. Samadanam, R. Mareeswaran, A. Suyavaran, M.S. Kumar, K. Premkumar, C. Thirunavukkarasu, *Colloid. Surf. B*, 102 (2013) 808–815.
28. Z. Krpetic, G. Scari, E. Caneva, G. Speranza, F. Porta, *Langmuir*, 25 (2009) 7217–7221.
29. M.V. Sujitha, S. Kannan, *Spectrochim. Acta A*, 102 (2013) 15–23.
30. D.D. Mubarak Ali, N. Thajuddin, K. Jeganathan, M. Gunasekaran, *Colloid. Surf. B*, 85 (2011) 360–365.
31. S.K. Basha, K. Govindaraju, R. Manikandan, J.S. Ahn, E.Y. Bae, G. Singaravelu, *Colloid. Surf. B*, 75 (2010) 405–409.
32. K.P. Kumar, W. Paul, C.P. Sharma, *Process Biochem*, 46 (2011) 2007–2013.
33. M. Noruzi, D. Zare, D. Davoodi, *Spectrochim. Acta A*, 94 (2012) 84–88.
34. Y. Xu, Y. Qin, S. Palchoudhury, U. Bao, *Langmuir*, 27 (2011) 8990–8997.
35. C. Fang, N. Bhattarai, C. Sun, and M. Zhang, *Small*, 5 (2009) 1637–1641.
36. N.F. Chiu, T.Y. Huang, *Sensors and Actuators B; chemical*, 197 (2014) 35–42.
37. H. He, J. Klinowski, M. Forster, A. Lerf, *Chem. Phys. Lett*, 287 (1998) 53–56.
38. A. Lerf, H. He, M. Forster, J. Klinowski, *J. Phys. Chem. B* 102 (1998) 4477–4482.
39. K.H. Liao, Y.S. Lin, C.W. Macosko, C.L. Haynes, *ACS Appl. Mater. Interfaces*, 3(2011) 2607–2615.
40. B. Lu, T. Li, H. Zhao, X. Li, C. Gao, S. Zhang, E. Xie, *Nanoscale*, 4 (2012) 2978–2982.
41. O. Akhavan, E. Ghaderi, *J. Phys. Chem. C* 113 (2009) 20214 – 20220.
42. Y. Liu, D.S. Yu, C. Zeng, Z.C. Miao, L.M. Dai, *Langmuir*, 26 (2010) 6158–6160.
43. Q.Y. He, H.G. Sudibya, Z.Y. Yin, S.X. Wu, H. Li, F. Boey, W. Huang, P. Chen, H. Zhang, *ACS Nano*, 4 (2010) 3201–3208.
44. C. Xu, D. Yang, L. Mei, B. Lu, L. Chen, Q. Li, H. Zhu, T. Wang, *ACS Appl. Mater. Interfaces*, 5 (2013) 2715–2724.
45. W. S. Hummers and R. E. Offeman, *J. Am. Chem. Soc*, 80 (1958) 1339–1339.
46. R.K. Das, N. Gogoi, U. Bora, *Bio process Biosyst. Eng*, 34 (2011) 615–619.
47. M.M.H. Khalil, E.H. Ismail, F. El-Magdoub, *Arabian J. Che*, 5 (2012) 431–437.

48. K. Saravanakumar, M. M. Ramjan, P. Suresh, V. Muthuraj, *J. Alloys Compd*, 664 (2016) 149-160.
49. R. M. Resendez, N. O. Nunez, E. D. B. Castro, C. Luna, *RSC Adv*, 3 (2013) 20765-20771.
50. M. Zargar, K. Shameli, G. R. Najafi, F. Farahan, *Journal of Industrial and Engineering Chemistry*, 20 (2014) 4169-4175.
51. P. Muthukrishnan, K. Saravanakumar, B. Jeyaprabha, P. Prakash, *Metallurgical and Materials Transactions A*, 45 (2014) 4510-4525.
52. S. Mukherjee, V. Sushma, S. Patra, A. K. Barui, M. P. Bhadra, B. Sreedhar, C. R. Patra, *Nanotechnology*, 23 (2012) 455103.
53. J. Lin, X. Wang, G. Shen, D. Cui, *Journal of Nanomaterials*, 2016 (2016) 1-8
54. I. Streeter, G. G. Wildgoose, L. Shao, R. G. Compton, *Sens. Actuators B; chemical*, 133 (2008) 462-466.
55. S. Thiagarajan, R. F. Yang, S. M. Chen, *Bioelectrochemistry*, 75 (2009) 163-169.
56. L. Zhang, L. Ning, S. Li, H. Pang, Z. Zhang, H. Ma, H. Yan, *RSC Adv*, 6 (2016) 66468-66476.
57. J. Zhao, Y. H. Yu, B. Weng, W. M. Zhang, A. T. Harris, A. I. Minett, Z. L. Yue, X. F. Huang, J. Chen, *Electrochem. Commun*, 37 (2013) 32-35.
58. F. Gao, X. L. Cai, X. Wang, C. Gao, S. L. Liu, F. Gao and Q. X. Wang, *Sens. Actuators, B*, 186 (2013) 380-387.
59. X. F. Liu, L. Zhang, S. P. Wei, S. H. Chen, X. Ou and Q. Y. Lu, *Biosens. Bioelectron*, 57 (2014) 232-238.
60. S. Palanisamy, S. Ku and S. M. Chen, *Microchim. Acta*, 180 (2013) 1037-1042.
61. X. F. Liu, S. P. Wei, S. H. Chen, D. H. Yuan and W. Zhang, *Biochem. Biotechnol*, 173 (2014) 1717-1726.
62. X. Weng, Q. X. Cao, L. X. Liang, J. R. Chen, C. P. You, Y. M. Ruan, H. J. Lin and L. J. Wu, *Talanta*, 117 (2013) 359-365.
63. S. Chen, W. Yang, X. Chen, *Electroanalysis*, 22 (2010) 908-911.
64. A. J. Wang, J. Feng, Y. F. Li, J. L. Xi, W. J. *Microchim Acta*, 171 (2010) 431-436.
65. D. B. Gorle and M. A. Kulandainathan, *RSC Adv*, 6 (2016) 19982-19991